Multi-fault earthquakes with kinematic and geometric rupture complexity: how common?

Conference Paper · November 2017

4 authors:

Mark Cameron Quigley
University of Canterbury

Hiwa Mohammadi
University of Melbourne

Abigail Jiménez
Others

Brendan Gilbert Duffy
University of Melbourne

INQUA Focus Group Earthquake Geology and Seismic Hazards

paleoseismicity.org

Multi-fault earthquakes with kinematic and geometric rupture complexity: how common?

Quigley, Mark (1,2), Mohammadi, Hiwa (1), Jiménez, Abigail (3) Duffy, Brendan (1)

(1) School of Earth Sciences, The University of Melbourne, Parkville VIC 3010, Australia
(2) Department of Geological Sciences, University of Canterbury, New Zealand
(3) Departamento de Química y Física, Universidad de Almería, Carretera de Sacramento s/n, Almería, Spain

Abstract: *We examine 257 finite-fault rupture models for 135 moment magnitude (M_w) 4.1 to 8.1 continental earthquakes to estimate how many source faults ruptured in each earthquake. We use fault geometries and rupture kinematic criteria to estimate fault populations. The minimum observed M_w for multi-fault rupture is 6.0. Approximately ~37% of the 135 earthquakes investigated were sourced from multi-fault ruptures. Upper-bounds and variance of fault rupture populations increase with increasing M_w. Fault rupture populations show no dependency on strain rate or proximity to plate boundaries. Coulomb stress modelling provides useful insights into why many earthquakes exhibit complex multi-fault rupture characteristics, and how this influences earthquake M_w maximum estimations and shapes of earthquake frequency-magnitude distributions. The 2016 M_w 7.8 Kaikoura earthquake is amongst the most complex multi-fault earthquakes ever recorded.*

Key words: *multi-fault earthquakes, rupture complexity, earthquake catalogues*

INTRODUCTION

Many continental earthquakes, including the 2016 M_w 7.8 Kaikoura and 2010 M_w 7.1 Darfield earthquakes, are sourced from the concurrent rupture of multiple faults with different orientations, rupture kinematics, and source Mw contributions (e.g., Hamling et al., 2017; Beavan et al., 2012). Here we ask, *how globally common are multi-fault earthquake ruptures, and why do they occur*?

To address these questions, we must first distinguish a "single earthquake" emanating from a spatiotemporally defined source from multiple earthquakes separated in time and / or space. Temporal gaps in seismic moment release rate exceeding 20 seconds are interpreted as distinct earthquakes (≤ 20 second gaps are interpreted as a single earthquake). Fault ruptures with the most proximal subsurface rupture termini exceeding 10 km apart are classified as distinct earthquakes (≤ 10 km gaps are interpreted as a single earthquake source). These criteria allow us to distinguish a defined multi-fault earthquake from multiple fault ruptures (multiple earthquakes) with intervening non-rupturing periods indicated by moment release rate gaps that may be 10s of seconds or hours apart, such as the 1986 Tennant Creek (Bowman 1992) and 2010-2011 Canterbury earthquake sequences (Quigley et al., 2016) and (ii) dynamically-triggered earthquakes on distal fault systems that occur quasi-instantaneously with the mainshock but that are not structurally or kinematically linked to the mainshock source fault(s) (Nissen et al., 2016).

We define a distinct "fault" using two different sets of criteria that incorporate structural and kinematic components of the rupture source. A *geometrically distinct* fault deviates at its termini by ≥ 20 degrees in strike and / or ≥ 20 degrees in dip from the termini of its nearest neighbouring faults. A *kinematically distinct* fault is distinguished by abrupt changes of ≥ 30 degrees in the slip vector (rake and / or azimuth) from neighbouring faults. We also count the number of distinct slip patches (i.e., asperities) with minimum slip values ≥ 1 m that taper outwards to encircling low slip domains in the source models, although we do not explicitly consider these in the fault population analyses presented herein

We first downloaded 197 seismic source models for 92 different earthquakes from the SRCmod Catalogue (http://equake-rc.info/SRCMOD/) (Mai and Thingbaijam, 2014) from June 1 to August 1, 2017. All original publication sources were consulted to confirm the reliability of the source models in the database. A further 60 source models for 43 different earthquakes were obtained using Google Scholar and Scopus searches for "earthquake source model" over the same time interval. Earthquakes dates are between April 1906 and June 2017 and corresponding source models were published between 1982 and 2017. For earthquakes where multiple source models and fault populations exist, we selected a preferred model based on the perceived quality and quantity of data used to derive the source model. Models were typically given the higher preference if they included InSAR, GPS and near-source seismicity data (e.g., strong ground motion data) that allowed rupture complexity to be investigated in higher fidelity than models where teleseismic data was the primary input. Our dataset should be viewed as preliminary; we are continuously searching for missing events and additional source models to gain further clarity on this topic.

DISCUSSION

Reported fault populations for individual earthquakes and for the overall catalogue typically exceed fault populations that can be distinguished kinematically and geometrically (Figure 1). The upper-bound for the number of reported faults in the catalogue seems to increase with increasing year of publication (Figure 2). This could relate to the emergence and increasing utility of new technologies (e.g., InSAR) that enabled multi-fault earthquake ruptures to be better identified, or it could relate to changes in the abundance of multi-fault earthquakes. The first use of InSAR to identify fault ruptures (Massonnet et al., 1993 – not pictured in Figure 2) led to increasing utility of this technique; many post-2000 multi-fault earthquake models in the catalogue were developed using InSAR (Figure 2). The low relative abundance of M_w>7 earthquakes in the early (pre-2000) part of the catalogue (Figure 3) prohibits us from directly evaluating whether the apparent increase in upper bounds of fault populations reflects the increasing population of large earthquakes for which rupture models were published, and / or an increased occurrence of multi-fault earthquakes.

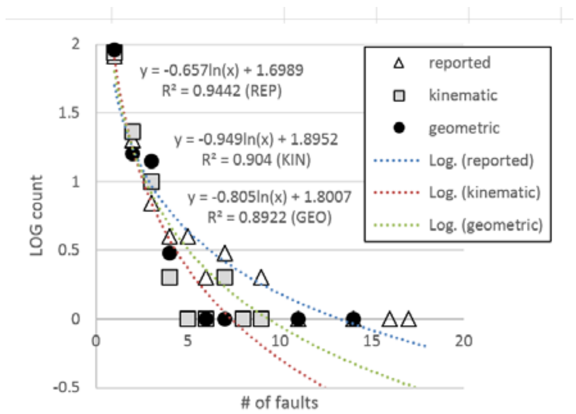

Figure 1: Number of distinct faults (LOG count of preferred value) for 128 earthquakes as reported in literature (REP), distinguished kinematically (KIN), and distinguished geometrically (GEO).

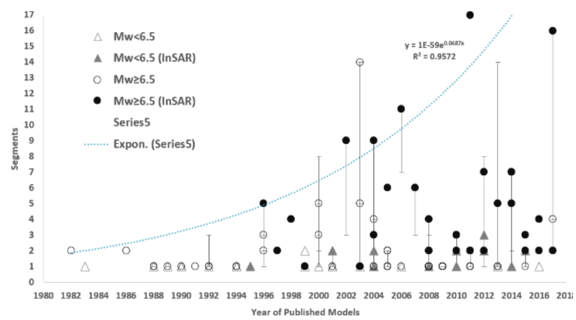

Figure 2: Number of reported faults ('segments') versus published year of preferred source model. Dotted line denotes exponential fit through six earthquakes with largest segment populations.

The smallest M_w multi-fault earthquake based on either kinematic or geometric criteria is 6.0 (Figure 4,5). This could reflect a reduced ability to resolve multi-fault earthquake ruptures at lower M_w and/or an increased likelihood that lower Mw earthquakes are confined to single fault sources. The upper range of fault populations increases with increasing M_w (Figures 4,5). Approximately 37% of the 135 earthquakes investigated were sourced from multi-fault ruptures. The number of earthquake source faults does not correlate clearly with strain rate (Figure 6) or distance from plate boundary (Figure 7).

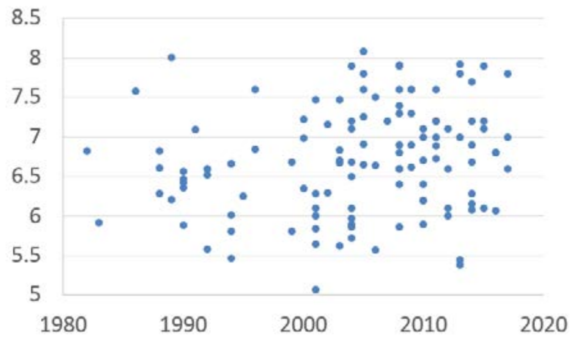

Figure 3: Earthquake M_w (y axis) versus publication year of preferred source model (x axis).

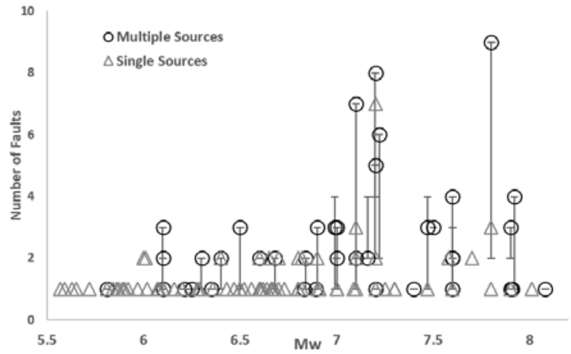

Figure 4: Kinematically-distinguished fault populations versus earthquake M_w.

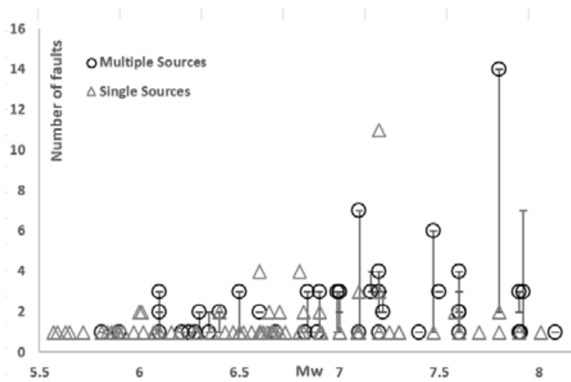

Figure 5: Geometrically-distinguished fault populations versus earthquake M_w.

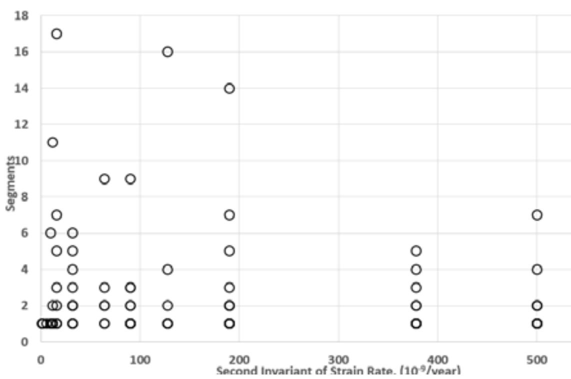

Figure 6: Strain rate versus reported fault segments

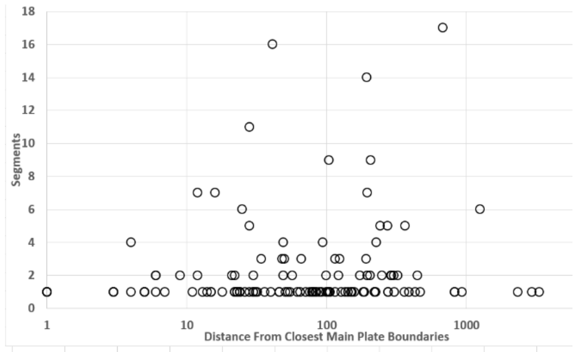

Figure 7: Distance from plate boundary versus reported fault segments.

Our Coulomb stress modelling (Figure 8) of the source faults for the Darfield earthquake (from Beavan et al., 2012) reveals one reason why multi-fault earthquakes are common; static stress changes exerted on receiver faults following mainshock rupture (top panel) exceed rupture triggering thresholds, and these ruptures in turn trigger rupture on other adjacent faults (bottom panel), encouraging the rupture to cascade across the network.

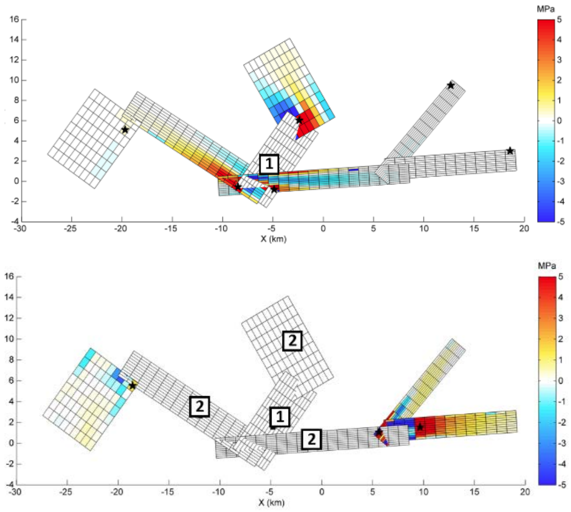

Figure 8: Coulomb stress modelling of the Darfield earthquake. Fault (1) denotes hypocentral source fault rupture. Faults (2) are receiver faults that rupture immediately after fault (1) due to imposed static stresses. Combined ruptures of (1) and (2) cause large positive static stress changes on the remaining faults, enabling rupture spreading across the entire fault network.

Multi-fault earthquakes result in an amalgamated M_w that exceeds the M_w of any contributing individual source fault (Figure 9). The maximum M_w of the fault system similarly exceeds the maximum M_w of any one contributing source. The shape of the Gutenberg-Richter frequency-M_w distribution is strongly influenced by multi-fault earthquakes. If the G-R *b* value derived from fits to lower Mw events is projected to higher magnitudes, the multi-fault earthquake scenario results in lower-than-expected Mw populations in the M_w ranges of the individual source faults, whereas the source de-aggregated Mw over-populates this Mw range.

The 2016 M_w 7.8 Kaikoura earthquake is perhaps the most kinematically and geometrically complex earthquake ever recorded (Hamling et al., 2017). However, aspects of this earthquake such as the ~25 km gap between adjacent ruptures (Kaiser et al., 2017) and possible dynamic triggering (Hollinsworth et al., 2017) raise complications on how this earthquake should be divided into distinct events with different fault populations. This remains a focus of further research. Other complex multi-fault earthquakes include the 2010 M_w 7.1 El Mayor-Cucapah, 2010 M_w 7.1 Darfield, 1997 M_w 7.2 Zirkuh (East Iran), and 1992 M_w 7.2 Landers earthquakes.

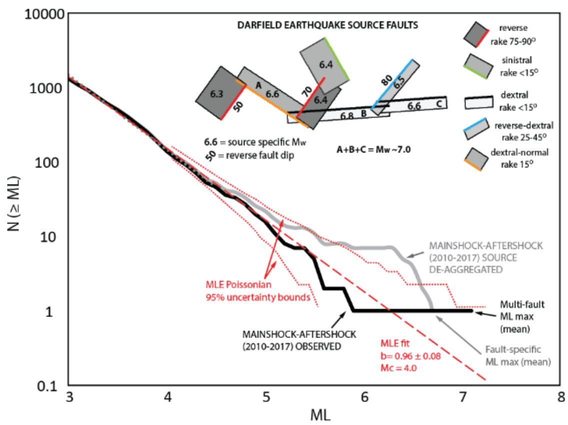

Figure 9: Geometrically-distinguished fault populations versus earthquake M_w.

REFERENCES

Bowman, J. R., 1992. The 1988 Tennant Creek, Northern Territory, earthquakes: A synthesis. *Australian Journal of Earth Sciences*, 39(5), 651-669.

Hamling, I.J., and 28 others, 2017. Complex multifault rupture during the 2016 Mw 7.8 Kaikōura earthquake, New Zealand. *Science*, 356(6334), p.eaam7194.

Hollinsworth, J., Ye, L., & Avouac, J. P., 2017. Dynamically triggered slip on a splay fault in the Mw 7.8, 2016 Kaikoura (New Zealand) earthquake. Geophysical Research Letters, 44(8), 3517-3525.

Kaiser, A., and 23 others, 2017. The 2016 Kaikōura, New Zealand, Earthquake: Preliminary Seismological Report. Seismological Research Letters, 88(3), 727-739.

Mai, P.M. and Thingbaijam, K.K.S., 2014. SRCMOD: An online database of finite-fault rupture models. Seismological Research Letters, 85(6), pp.1348-1357.

Massonnet, D., Rossi, M., Carmona, C., Adragna, F., Peltzer, G., Feigl, K. and Rabaute, T., 1993. The displacement field of the Landers earthquake mapped by radar interferometry. *Nature*, 364(6433), pp.138-142.

Nissen, E. K., Elliott, J. R., R. A. Sloan, T. J. Craig, G. J. Funning, A. Hutko, B. E. Parsons & T. J. Wright, 2016. Dynamic triggering of an earthquake doublet exposes limitations to rupture forecasting, *Nature Geoscience*, doi:10.1038/NGEO2653

Quigley, M.C., Hughes, M.W., Bradley, B.A., van Ballegooy, S., Reid, C., Morgenroth, J., Horton, T., Duffy, B. and Pettinga, J.R., 2016. The 2010–2011 Canterbury earthquake sequence: Environmental effects, seismic triggering thresholds and geologic legacy. *Tectonophysics*, 672, pp.228-274.